International Journal of Solids and Structures 51 (2014) 566–574

Contents lists available at ScienceDirect

International Journal of Solids and Structures

journal homepage: www.elsevier.com/locate/ijsolstr

Mechanics of adhesive contact at the nanoscale: The effect of surface stress

Xiang Gao [a], Feng Hao [b], Zhuping Huang [a], Daining Fang [a,*]

[a] LTCS and Department of Mechanics and Engineering Science, College of Engineering, Peking University, 100871, China
[b] Department of Engineering Mechanics, Tsinghua University, 100084, China

ARTICLE INFO

Article history:
Received 13 May 2013
Received in revised form 11 October 2013
Available online 23 October 2013

Keywords:
Adhesive contact
Surface effect
Pull-off force
Dimensional analysis
Scaling laws

ABSTRACT

At small length scales, the adhesion and surface effect are of great significance, both of which play important roles in the contact between two elastic solids. In this study, the classical Johnson–Kendall–Roberts (JKR) adhesive contact theory is generalized to the nanoscale at which the surface effect is considered. The influence of the surface stress on the JKR adhesive contact is investigated by employing the non-classical Boussinesq fundamental solutions. It is found that, compared with the classical theory, the pull-off force increases while the critical contact radius decreases as a result of the surface effect. Numerical results show that a relative error of 10% can be introduced in the pull-off force when the indenter radius is less than 20 nm. A detailed theoretical analysis of this interesting phenomenon is presented based on dimensional analysis, and two scaling laws for the adhesive contact at the nanoscale are constructed. These two new scaling laws reveal that the pull-off force is relevant to the elastic properties of the bulk materials, which is different from the classical adhesive contact theory. The present work is promising for the engineering applications in micro-electro-mechanical systems (MEMS) and nano-intelligent devices.

1. Introduction

Tremendous progresses have been made in nanotechnology in recent decade because of its promising applications in micro-electro-mechanical systems (MEMS) and nano-intelligent devices. For nano-structured materials, a growing body of research shows that several important physical properties, such as the elastic modulus (Chen et al., 2006; Jing et al., 2006), yield strength (Zhang et al., 2010), indentation hardness (Ma and Clarke, 1995; Feng and Nix, 2004) and melting temperature (Sun et al., 2002), become size-dependent; thus, determining how to interpret these interesting phenomena is being a hot point in solid mechanics and material science. At the nanoscale, the influence of the surface energy is of great importance because the surface to volume ratio is remarkably large for nanostructures, and quite a number of the size-dependent physical properties of nanosized materials can be rationalized by invoking the concept of surface energy.

Many researchers have studied the mechanical behaviors of the nano-structured materials by employing the surface stress theory (Gurtin and Murdoch, 1975, 1978; Povstenko, 1993; Cammarata, 1994; Huang and Wang, 2006; Huang and Sun, 2007). Miller and Shenoy (2000) studied the size-dependent elastic properties of nanosized structural elements and constructed a simple model to predict the size dependence of the effective properties. Sharma and Ganti (2004) and Duan et al. (2005a) studied the eigenstrain problem of spherical inhomogeneities with the interface effect and concluded that the Eshelby tensor is size-dependent. Dingreville et al. (2005) constructed a framework to incorporate the surface free energy and derived the effective moduli of the nanosized structural elements. Duan et al. (2005b) studied the effective elastic constants of composites that contained spherical nano-inhomogeneities with interface stress but they only considered the effect of the interface elasticity. Later, Huang and Sun (2007) established a micromechanical scheme to predict the effective modulus of nanocomposites, in which both the effect of the residual interface stress and the interface elasticity can be taken into account. It was shown that Duan et al. (2005b)'s result is just a special case of Huang and Sun (2007). Park and Klein (2008) investigated the surface stress effect on the resonant properties of nanowires and emphasized the importance of the residual surface stress. Dingreville and Qu (2008) derived a new relation between the interfacial excess energy and the interfacial excess stress for planar interfaces, which can account for both the in-plane and transverse deformations of the real material interfaces. Recently, several new directions in the surface effect have been explored. For example, the mechanics of rough surfaces and its applications were studied (Weissmuller and Duan, 2008; Mohammadi et al., 2013); the curvature dependence of the surface energy was considered to investigate its significance on nanostrucutres (Chhapadia et al., 2011;

* Corresponding author. Tel.: +86 10 62760322 (O); fax: +86 10 62751812.
E-mail address: fangdn@pku.edu.cn (D. Fang).

0020-7683/$ - see front matter © 2013 Elsevier Ltd. All rights reserved.
http://dx.doi.org/10.1016/j.ijsolstr.2013.10.017

Mohammadi and Sharma, 2012); the surface effects were found to strongly influence the electromechanical coupling behaviors of nano-materials (Dai et al., 2011; Dai and Park, 2013).

There has been some preliminary research in contact mechanics at the nanoscale. Wang and Feng (2007) studied the two dimensional half-space problems with the effect of the residual surface stress. Long et al. (2012) studied the effect of the residual surface stress on the two dimensional Hertzian contact problem, and later Long and Wang (2013) generalized their work to the three dimensional case. Zhao and Rajapakse (2009) studied the influence of the surface elasticity on the surface-loaded isotropic elastic layers. It has been demonstrated that the residual surface stress and the surface elasticity are two equally important aspects in the surface effect, but only one of these effects is considered in the above-mentioned works. Gao et al. (2013) established a non-classical formulation of the Boussinesq problem, in which both the residual surface stress and the surface elasticity were considered, and constructed a three dimensional Hertzian contact model with the surface effect. However, the contact models reviewed above are only concerned with the Hertzian contact model. In fact, the Van der Waals interaction between the ideal surfaces of two solids will result in the adhesion between elastic bodies. Thus, the adhesion effect is truly a surface/interface phenomenon. When it comes to the elastic contact problems at the nano- or microscale, the adhesion should be an indispensable factor (Zhao et al., 2003).

The pioneering work in the adhesive contact can be traced back to Bradley (1932), who first solved the adhesive contact between a rigid sphere and a rigid plane and gave the formula of the pull-off force. The theory of the adhesive contact between two elastic bodies was first established by Johnson et al. (1971) in their eponymous Johnson–Kendall–Roberts (JKR) theory, which is based on the balance between the elastic energies and the work of adhesion. The JKR theory predicted a compressive stress field near the central region of contact and a singular tensile stress field near the contact edges. On the other hand, Derjaguin et al. (1975) developed an alternative adhesive contact theory (Derjaguin–Muller–Toporov theory or DMT theory), in which the stress field keeps in the Hertz profile within the contact region while the intermolecular adhesion outside the contact region is considered. Later, it was pointed out by Tabor (1977) that the JKR model is more suitable for the contact between relatively large and soft bodies while the DMT theory is more suitable for the contact between small and rigid bodies. Maugis (1992) developed a more general theory describing the transition between the JKR and DMT theories by using the Dugdale model. There has been extensive research that is based on these profound and significant adhesive contact theories. For example, a generalized adhesive contact model that considered the influence of shot-range and long-range attractive forces both inside and outside the actual contact area was developed (Schwarz, 2003); the classical JKR theory was extended to anisotropic materials and a model of reversible adhesion was developed (Chen and Gao, 2007); the adhesive behavior of the power-law graded materials was studied (Chen et al., 2009a,b); the adhesion of the nanoscale asperities with power-law profiles was investigated (Zheng and Yu, 2007; Grierson et al., 2013). It should be noted that there are substantial significant results on the adhesive contact in the literature, but regretfully, we can only review a small part of them here. The reader may refer to Barthel (2008) for a review of the adhesive interactions in contact mechanics. At the small length scales, both the adhesion and the surface stress play important roles in MEMS and nano-intelligent devices. However, to the authors' knowledge, the effect of surface stress on the adhesive contact between elastic bodies at the nanoscale has not been studied.

The objective of the present paper is to generalize the classical JKR adhesive contact model to the nanoscale by considering the surface effect and investigate the influence of the surface stress on the adhesive contact. The non-classical Boussinesq fundamental solutions developed by the authors in a previous paper (Gao et al., 2013) are employed to formulate this non-classical adhesive contact model. It is found that, compared with the classical theory, the pull-off force increases while the corresponding critical contact radius decreases as a result of the surface effect. A detailed theoretical study of these significant phenomena is presented and two scaling laws are constructed based on dimensional analysis. These new scaling laws describe the characteristics of the adhesive contact at the nanoscale. It should be mentioned that, for simplicity, the surface roughness is not considered in the present work.

This paper is organized as follows. The basic theoretical framework of the JKR adhesive contact model with the surface effect is formulated in Section 2. The numerical results of the developed theory are illustrated in Section 3. The scaling laws of the pull-off force and the relevant critical contact radius are constructed in Section 4 using the dimensional analysis. The conclusions are summarized in Section 5.

2. Basic theory

The goal of this section is to generalize the classical JKR adhesive contact theory to the nanoscale by considering the surface effect. The non-classical Boussinesq solutions are given first as the preliminary, and then the basic theoretical framework of the JKR theory with the surface effect are formulated.

2.1. Non-classical Boussinesq solutions

The fundamental solutions of the Boussinesq problem play an important role in contact mechanics. At the nanoscale, a non-classical formulation of the Boussinesq problem with the surface stress effect was developed by Gao et al. (2013). In the three-dimentional Boussinesq problem, the normal displacement solution with the surface effect under axisymmetric normal pressure $p(r)$ is

$$u_z = \frac{1}{2\mu}\int_0^\infty \frac{\overline{p}(\xi)}{g(\xi)}[2(4\nu-3)k\xi + 8(\nu-1) - 2(k\xi+2)\xi z]e^{-z\xi}J_0(\xi r)\mathrm{d}\xi, \tag{1}$$

where μ and ν are the shear modulus and the Poisson ratio of the material, respectively, $J_0(\xi r)$ denotes the zero order Bessel function of the first kind and

$$\overline{p}(\xi) = \int_0^\infty rp(r)J_0(\xi r)\mathrm{d}r \tag{2}$$

is the Hankel transformation of the normal pressure $p(r)$. The function $g(\xi)$ is expressed as

$$g(\xi) = -4 + 4(\nu-1)(k+l)\xi + (4\nu-3)kl\xi^2 \tag{3}$$

and l and k are two intrinsic length scales, which reflect the surface effect and are defined as

$$l = \frac{\sigma_0}{\mu}, \quad k = \frac{\gamma_1^* + \gamma_1}{\mu}, \tag{4}$$

where σ_0 denotes the residual surface stress and γ_1^*, γ_1 are elastic constants of the material surface. For details, the reader may refer to the references by Huang's group (Huang and Wang, 2006, 2013; Huang and Sun, 2007).

Putting $z = 0$ in the Eq. (1), we obtain the surface displacement under normal pressure:

$$\overline{u}_z(r) = \frac{1}{2\mu}\int_0^\infty \overline{p}\left(\frac{t}{a}\right)\frac{2(4\nu-3)k_r t + 8(\nu-1)}{g(t;l_r,k_r)}J_0\left(\frac{r}{a}t\right)\mathrm{d}t, \tag{5}$$

where we use the variable substitution $t = a\xi$ in the integral. As a result, the function $g(t; l_r, k_r)$ is in the form

$$g(t; l_r, k_r) = -4 + 4(v-1)(k_r + l_r)t + (4v-3)k_r l_r t^2 \tag{6}$$

and l_r, k_r are two dimensionless surface parameters, which are defined as

$$l_r = \frac{l}{a}, \quad k_r = \frac{k}{a}. \tag{7}$$

Generally, the geometrical parameter a denotes the contact radius in the normal contact problems.

By using the fundamental solution (5), the normal surface displacement under the Hertz pressure

$$p(r) = \frac{p_1}{a}\sqrt{a^2 - r^2} \quad (0 \leqslant r \leqslant a) \tag{8}$$

can be expressed as

$$\overline{u}_{z1}(r) = \frac{p_1 a}{2\mu}\int_0^\infty \left[-\frac{\cos t}{t^2} + \frac{\sin t}{t^3}\right]\frac{2(4v-3)k_r t + 8(v-1)}{g(t; l_r, k_r)} J_0\left(\frac{r}{a}t\right)\mathrm{d}t, \tag{9}$$

where p_1 is the maximum pressure in the contact region. If the pressure is in the form

$$p(r) = \frac{p_0 a}{\sqrt{a^2 - r^2}} (0 \leqslant r \leqslant a), \tag{10}$$

the related normal displacement is

$$\overline{u}_{z0}(r) = \frac{p_0 a}{2\mu}\int_0^\infty \left[\frac{\sin t}{t}\right]\frac{2(4v-3)k_r t + 8(v-1)}{g(t; l_r, k_r)} J_0\left(\frac{r}{a}t\right)\mathrm{d}t, \tag{11}$$

where p_0 also denotes the maximum pressure in the contact region. Noting that if the surface effect is neglected, i.e., $l_r = k_r = 0$, the surface displacements in Eqs. (9) and (11) reduce to the classical results (Johnson, 1985).

2.2. The JKR adhesive contact model with the surface effect

In this part, we are going to formulate the JKR adhesive contact model with the surface effect. Assuming that a rigid spherical indenter with radius R is pressed into an isotropic elastic half-space, the interaction pressure in the contact region, according to the JKR theory, is a superposition of the Hertz pressure (8) and the pressure (10):

$$p(r) = \frac{p_0 a}{\sqrt{a^2 - r^2}} + \frac{p_1}{a}\sqrt{a^2 - r^2}. \tag{12}$$

In the JKR adhesive contact model, the boundary condition for the normal displacement within the contact region is

$$\overline{u}_z = \delta - \frac{r^2}{2R}, \tag{13}$$

where δ is the mutual approach of distant points in the two solids. $\overline{u}_z(r)$ is the surface normal displacement under the contact pressure (12); thus, according to the superposition principle of displacements, $\overline{u}_z(r)$ can be expressed as

$$\overline{u}_z(r) = \delta - \frac{r^2}{2R} = \overline{u}_{z0}(r) + \overline{u}_{z1}(r). \tag{14}$$

Substituting Eqs. (9) and (11) into Eq. (14), we obtain the following non-classical load–displacement relation

$$\begin{aligned}\delta - \frac{r^2}{2R} = {} & \frac{p_0 a}{2\mu}\int_0^\infty \left[\frac{\sin t}{t}\right]\frac{2(4v-3)k_r t + 8(v-1)}{g(t; l_r, k_r)} J_0\left(\frac{r}{a}t\right)\mathrm{d}t \\ & + \frac{p_1 a}{2\mu}\int_0^\infty \left[-\frac{\cos t}{t^2} + \frac{\sin t}{t^3}\right]\frac{2(4v-3)k_r t + 8(v-1)}{g(t; l_r, k_r)} J_0\left(\frac{r}{a}t\right)\mathrm{d}t,\end{aligned} \tag{15}$$

which takes into account the surface effect.

In the classical case (Johnson, 1985), the surface normal displacement induced by the Hertz pressure (8) is a quadratic function of variable r and the pressure (10) gives rise to a uniform normal displacement in the contact region. Thus, by taking the Taylor series expansion of the right side of Eq. (15) with respect to variable r, keeping $\overline{u}_{z1}$ up to the quadratic term and keeping $\overline{u}_{z0}$ up to the constant term, we can obtain the approximate load–displacement relation

$$\delta - \frac{r^2}{2R} \doteq \frac{p_0 a}{2\mu} I(a) + \frac{p_1 a}{2\mu} F(a) - \frac{p_1 r^2}{8\mu a} G(a), \tag{16}$$

where

$$\begin{aligned} F(a) &= \int_0^\infty \left[-\frac{\cos t}{t^2} + \frac{\sin t}{t^3}\right]\frac{2(4v-3)k_r t + 8(v-1)}{g(t; l_r, k_r)}\mathrm{d}t, \\ G(a) &= \int_0^\infty \left[-\cos t + \frac{\sin t}{t}\right]\frac{2(4v-3)k_r t + 8(v-1)}{g(t; l_r, k_r)}\mathrm{d}t, \\ I(a) &= \int_0^\infty \left[\frac{\sin t}{t}\right]\frac{2(4v-3)k_r t + 8(v-1)}{g(t; l_r, k_r)}\mathrm{d}t, \end{aligned} \tag{17}$$

are three functions of the contact radius a and reflect the surface effect. Hence, Eq. (16) results in

$$\delta = \frac{p_0 a}{2\mu} I(a) + \frac{p_1 a}{2\mu} F(a), \quad \frac{1}{2R} = \frac{p_1}{8\mu a} G(a) \tag{18}$$

and then we can solve for p_0 and p_1, which can be expressed as

$$p_0 = \frac{2\mu}{I(a)}\left(\frac{\delta}{a} - \frac{2a}{R}\frac{F(a)}{G(a)}\right), \quad p_1 = \frac{4\mu a}{RG(a)}. \tag{19}$$

When the surface effect is neglected (i.e., $l = k = 0$), we have

$$F(a) = \frac{1}{2}\pi(1-v), \quad G(a) = I(a) = \pi(1-v) \tag{20}$$

and Eqs. (19) will reduce to the results given by the classical JKR adhesive contact theory.

Notably, Eqs. (19) contain three unknown quantities: p_0, p_1 and a (for a given mutual approach δ). Thus, in order to determine the stress and strain states in the elastic half-space, there needs additional constraint condition: the total energy of the system reaches its minimum at equilibrium for a given mutual approach δ.

The total energy U_{tot} of this system is made up of two terms, the stored elastic energy U_{el} and the work of adhesion U_{ad}. The elastic strain energy stored in the bodies can be calculated by the work of the contact pressure

$$\begin{aligned} U_{el} &= \frac{1}{2}\int_A p(r)\overline{u}_z(r)\mathrm{d}A \\ &= \pi\int_0^a \left[p_0\left(1 - \frac{r^2}{a^2}\right)^{-1/2} + p_1\left(1 - \frac{r^2}{a^2}\right)^{1/2}\right]\left(\delta - \frac{r^2}{2R}\right) r\mathrm{d}r, \end{aligned} \tag{21}$$

which is easily shown to be

$$U_{el} = \pi a^2\left[p_0\left(\delta - \frac{1}{3}\frac{a^2}{R}\right) + p_1\left(\frac{1}{3}\delta - \frac{1}{15}\frac{a^2}{R}\right)\right]. \tag{22}$$

Therefore, the substitution of the Eqs. (19) into the Eq. (22) finally results in

$$\begin{aligned} U_{el} = {} & \frac{2\pi\mu}{I(a)} a\delta^2 + \frac{2\pi\mu a^3\delta}{R}\left[\frac{2}{3}\frac{1}{G(a)} - \frac{1}{I(a)}\cdot\left(\frac{2F(a)}{G(a)} + \frac{1}{3}\right)\right] \\ & + \frac{4}{3}\frac{\pi\mu a^5}{R^2}\frac{1}{G(a)}\left(\frac{F(a)}{I(a)} - \frac{1}{5}\right). \end{aligned} \tag{23}$$

The work of adhesion is given by

$$U_{ad} = -\pi a^2 \Delta\gamma, \tag{24}$$

where $\Delta\gamma$ is the energy of adhesion of both surfaces, and is defined as

$$\Delta\gamma = \gamma_1^s + \gamma_2^s - \gamma_{12}, \tag{25}$$

where γ_1^s, γ_2^s are the surface energy of both solid surfaces and γ_{12} is the interface energy.

Thus, the total energy U_{tot} of the system is

$$U_{tot} = U_{el} + U_{ad} = \frac{2\pi\mu}{I(a)} a\delta^2 + \frac{2\pi\mu a^3 \delta}{R}\left[\frac{2}{3}\frac{1}{G(a)} - \frac{1}{I(a)}\cdot\left(\frac{2F(a)}{G(a)} + \frac{1}{3}\right)\right] + \frac{4}{3}\frac{\pi\mu a^5}{R^2}\frac{1}{G(a)}\left(\frac{F(a)}{I(a)} - \frac{1}{5}\right) - \pi a^2 \Delta\gamma. \tag{26}$$

Equilibrium ensues when

$$\frac{\partial U_{tot}}{\partial a} = \frac{\partial U_{el}}{\partial a} + \frac{\partial U_{ad}}{\partial a} = 0, \quad \frac{\partial^2 U_{tot}}{\partial a^2} > 0. \tag{27}$$

This is equivalent to

$$2\pi\mu\delta^2\left(\frac{a}{I(a)}\right)' + \frac{2\pi\mu\delta}{R}\left[\frac{2}{3}\frac{a^3}{G(a)} - \frac{a^3}{I(a)}\cdot\left(\frac{2F(a)}{G(a)} + \frac{1}{3}\right)\right]' + \frac{4}{3}\frac{\pi\mu}{R^2}\left[\frac{a^5}{G(a)}\left(\frac{F(a)}{I(a)} - \frac{1}{5}\right)\right]' = 2\pi a\Delta\gamma, \tag{28}$$

where $(\cdot)'$ denotes the partial derivative with respect to the variable a. Therefore, we can solve for

$$\delta = \frac{-B \pm \sqrt{B^2 - 4AC}}{2A}, \tag{29}$$

where

$$A = \left(\frac{a}{I(a)}\right)', B = \frac{1}{R}\left[\frac{2}{3}\frac{a^3}{G(a)} - \frac{a^3}{I(a)}\cdot\left(\frac{2F(a)}{G(a)} + \frac{1}{3}\right)\right]', \quad C = \frac{2}{3}\frac{1}{R^2}\left[\frac{a^5}{G(a)}\left(\frac{F(a)}{I(a)} - \frac{1}{5}\right)\right]' - \frac{a\Delta\gamma}{\mu}. \tag{30}$$

Further, it can be concluded that the negative sign should be taken in Eq. (29) for a stable equilibrium by examining the second differential of the total energy.

The contact force can be calculated by Popov (2010)

$$F = \frac{dU_{tot}}{d\delta} = \frac{2\pi\mu}{I(a)}\left[2a\delta - \frac{a^3}{R}\left(\frac{2F(a)}{G(a)} - \frac{2}{3}\frac{I(a)}{G(a)} + \frac{1}{3}\right)\right]. \tag{31}$$

By substituting Eq. (29) into Eq. (31), we can obtain the relation between the contact force and the contact radius. The absolute value of the minimum contact force is defined as the pull-off force, denoted by F_A, and the corresponding contact radius is called the critical contact radius, denoted by a_c.

Exact analytical solutions of the pull-off force F_A and the critical radius a_c are unavailable when the surface stress effect is considered. In the following section, we will give a detailed numerical analysis about the effect of surface stress on the behaviors of adhesive contact.

3. Numerical results and discussions

In fact, the method we employed to take the surface stress effect into account in adhesive contact is to use the non-classical Boussinesq solutions in Eq. (15). In this study, only the normal displacement solutions with the surface effect are involved in Eq. (15). It is demonstrated in our former work (Gao et al., 2013) that this normal displacement is mainly influenced by the residual surface stress and the effect of the surface elasticity is less important. Thus, for simplicity, we neglect the surface elasticity (i.e., $k = 0$) and only consider the effect of residual surface stress on the adhesive contact in the following study. When the surface elasticity is neglected, the surface energy is approximately equal to the residual surface stress according to the Shuttleworth equation (Cammarata, 1994). The numerical results are presented for polymer EPMD (ethylene–propylene–diene monomer elastomers), which has a Poisson ratio of $\nu = 0.49$, a shear modulus of $\mu = 2$ MPa and a residual surface stress of $\sigma_0 = \gamma_1^s = 36$ mN/m (Mark, 2009). The indenter is assumed to be made of metal aluminum (Al), which has a residual surface stress of $\gamma_2^s = 2.3$ N/m (Medasani and Vasiliev, 2009). The energy of adhesion of both material surfaces can be estimated as $\Delta\gamma \approx 2\sqrt{\gamma_1^s\gamma_2^s} = 0.5755$ N/m (Popov, 2010). By substituting these material constants into the above analytical expressions, we can obtain the numerical results that are shown in the following figures. It should be noted that the corresponding physical quantities are nondimensionalized by the pull-off force F_{JKR}, the critical contact radius a_{JKR} and the critical mutual approach δ_{JKR} in the classical JKR adhesive contact theory, respectively, which are expressed as

$$F_{JKR} = \frac{3}{2}\pi\Delta\gamma R, \tag{32a}$$

$$a_{JKR} = \left(\frac{9}{8}\frac{\pi\Delta\gamma R^2}{E^*}\right)^{1/3}, \tag{32b}$$

$$\delta_{JKR} = -\left(\frac{3\pi^2\Delta\gamma^2 R}{64E^{*2}}\right)^{1/3}, \tag{32c}$$

where E^* is the equivalent elastic modulus:

$$E^* = \frac{E}{1-\nu^2} = \frac{2\mu}{1-\nu} \tag{33}$$

and E is the Young's modulus of the material.

Fig. 1 illustrates the variations of the contact force with the contact radius, and the result of the Hertz contact model with the surface effect is referenced from Gao et al. (2013). As shown in Fig. 1, due to the surface effect, an apparent increase in the contact force over that predicted by the classical JKR theory has been observed when the contact force is greater than zero ($F > 0$), which is in agreement with the results of the Hertz model. This phenomenon can be interpreted qualitatively by the impact of surface stress on the nanostructures. It has been concluded in the literature that the surface stress strengthens the contact stiffness of the material and the material surface becomes stiffer due to the surface effect (Long et al., 2012; Gao et al., 2013). Thus, it requires a greater contact force to generate the same contact radius as the classical case, and correspondingly, induces a smaller contact radius for the same contact force. In particular, because of the attractive forces act between material surfaces close together, an extra tensile force ($F < 0$ in Fig. 1) is required to separate two solid bodies placed in intimate contact. The minimum value of this required tensile force is called the pull-off force. Notably, compared with the classical JKR theory, the pull-off force becomes larger while the critical radius becomes smaller when the surface effect is taken into account.

The variations of the mutual approach with the contact radius are plotted in Fig. 2, which illustrates the influence of the residual surface stress on the mutual approaches in the Hertz theory and JKR theory. When the indenter is pressed into the material ($\delta > 0$), the mutual approach is greater than the classical result; and conversely, when the material surface is drawn towards the indenter due to the adhesion between solids ($\delta < 0$), the absolute

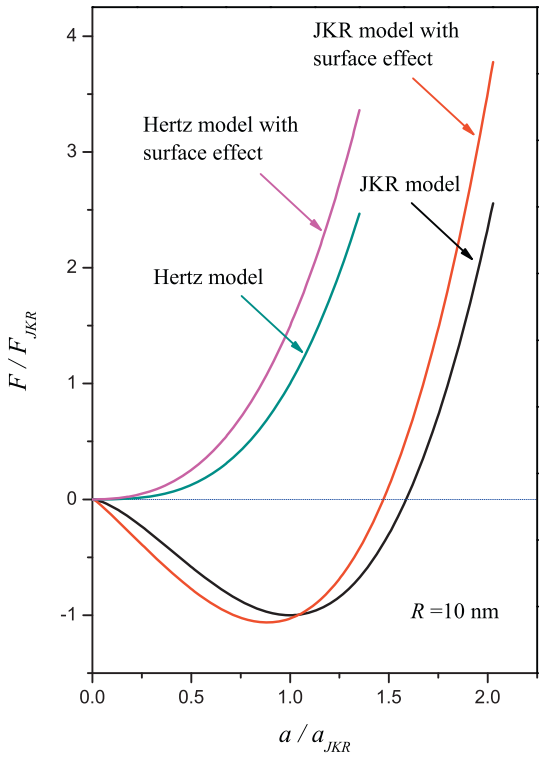

Fig. 1. The variation of the contact force with the contact radius.

value of the mutual approach becomes smaller compared with the classical result. This phenomenon can also be rationalized by the common view that the surface effect reinforces the contact stiffness of the materials at the nanoscale.

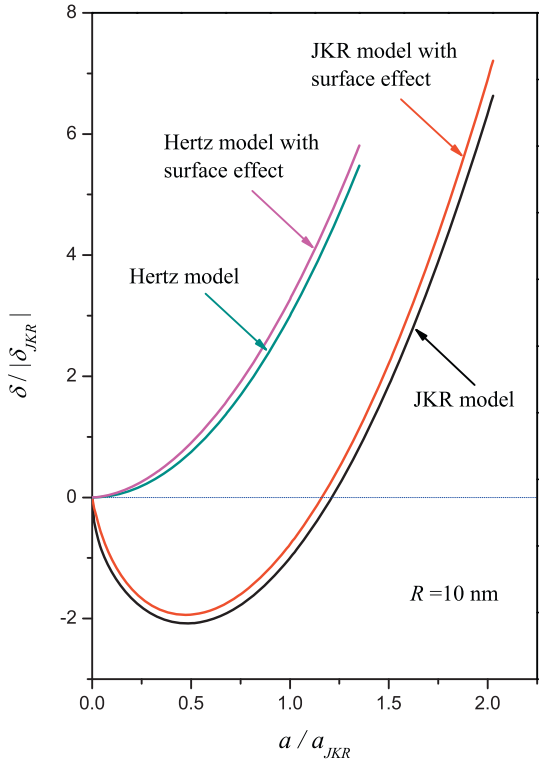

Fig. 2. The variation of the mutual approach with the contact radius.

Fig. 3 shows the relations between the contact force and the mutual approach, which reflects the influence of the residual surface stress on the elastic contact stiffness of materials. The elastic contact stiffness (H) is generally defined as the ratio of the contact force (F) to the mutual approach (δ), i.e., $H = F/\delta (F > 0)$. For the JKR model, the contact stiffness increases significantly due to the surface effect. This is in agreement with the case of the Hertz model. Moreover, the contact stiffness of the JKR model with the surface effect may exceed that of the classical Hertz model if the contact force is large enough. This indicates that the adhesive contact model with the surface effect is more applicable to the small-scale contact problems than the conventional contact models.

When the surface effect is considered at the nanoscale, the JKR adhesive contact model becomes size dependent. Fig. 4 clearly shows this feature, in which the contact force-contact radius relations are plotted for different indenter radii. Obviously, the solutions with the surface stress effect approach the classical JKR model as the indenter radius becomes larger.The variation of the incremental pull-off force ($\Delta F = F_A - F_{\mathrm{JKR}}$) with the indenter radius (R) is plotted in Fig. 5. The larger the indenter radius, the larger the incremental pull-off force. Remarkably, the pull-off force (F_A) depends nonlinearly on the indenter radius due to the surface effect, which is distinctly different from the classical results shown in Eq. (32a). The variation of the increment critical contact radius ($\Delta a = a_c - a_{\mathrm{JKR}}$) with the indenter radius (R) is shown in Fig. 6. It is interesting to note that the incremental critical radius tends to a constant while the indenter radius R is greater than 50 nm. A further analysis of these meaningful results will be given in the next section.

Fig. 7 and Fig. 8 illustrate in what range the surface effect becomes important and how large the surface effect should be. It can be concluded from both figures that the surface stress effect is significant when the indenter radius is smaller than 100 nm. Moreover, the $\Delta F/F_{\mathrm{JKR}}$ approach 10% and the $\Delta a/a_{\mathrm{JKR}}$ can reach 25% when the indenter radius is only a dozen of nanometers.

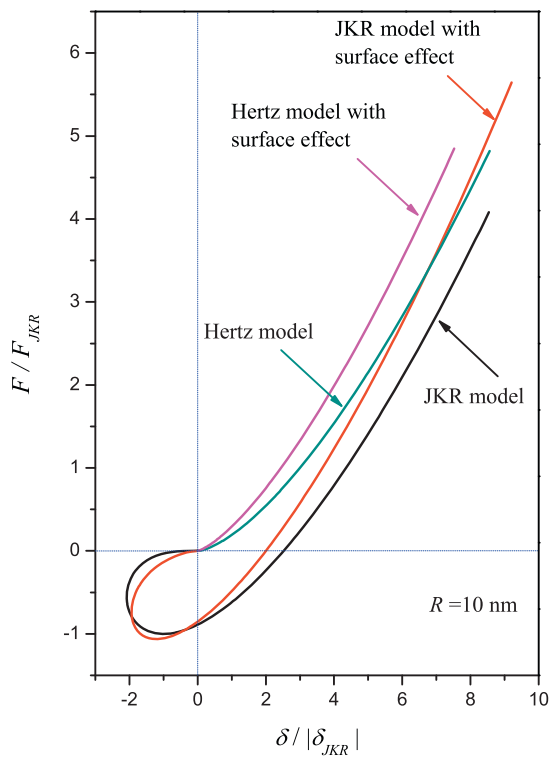

Fig. 3. The variation of the contact force with the mutual approach.

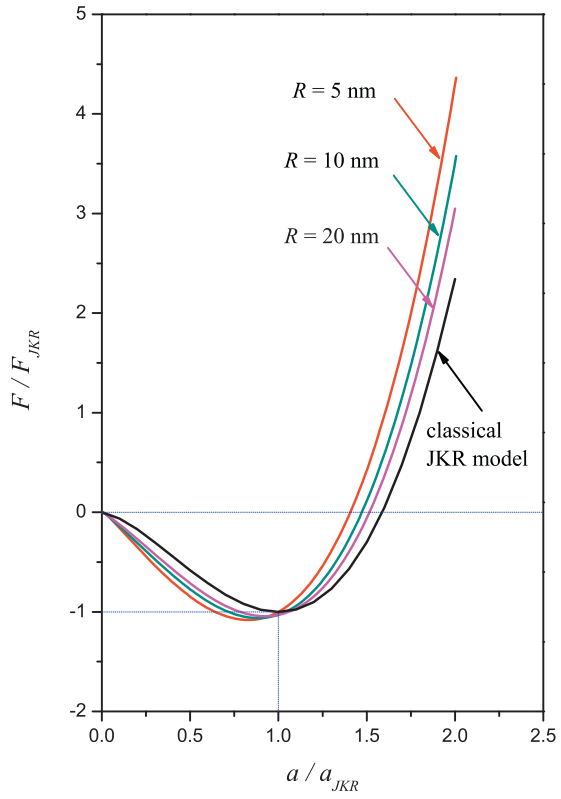

Fig. 4. The size dependence of the JKR adhesive model with the surface effect.

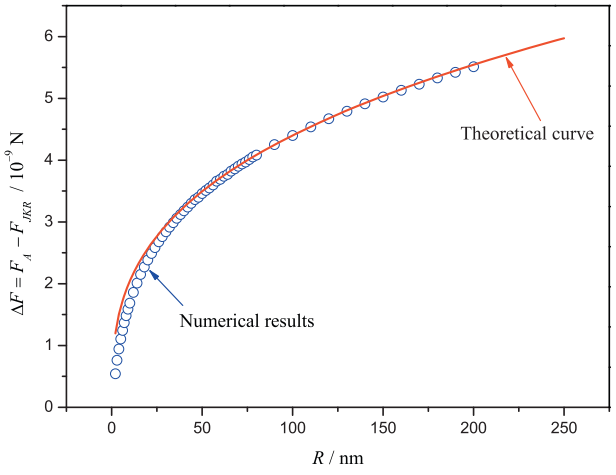

Fig. 5. The variation of the incremental pull-off force with the indenter radius.

4. Dimensional analysis and linear approximation

The quantities of interest in the adhesive contact are generally the pull-off force F_A and the corresponding critical contact radius a_c. The objective of this section is to construct the approximate analytical formulas for these two quantities using dimensional analysis.

4.1. Dimensional analysis of the pull-off force and the critical contact radius

The two dependent variables, F_A and a_c, must be functions, f and g, of the independent governing parameters, namely, the residual surface stress (σ_0), the energy of adhesion ($\Delta\gamma$), the indenter radius (R) and the equivalent elastic modulus (E^*):

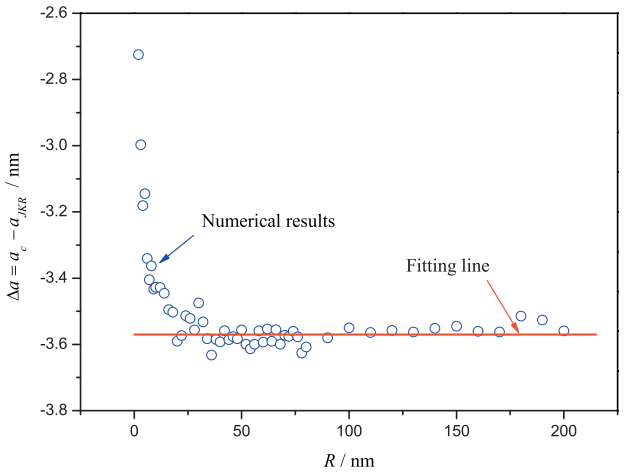

Fig. 6. The variation of the incremental critical radius with the indenter radius.

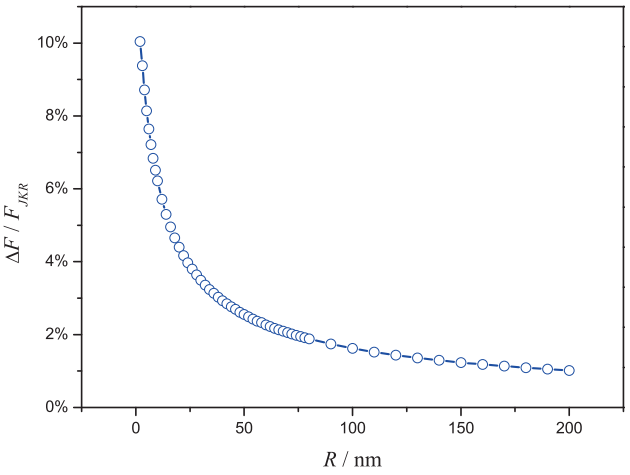

Fig. 7. The variation of the $\Delta F/F_{\mathrm{JKR}}$ with the indenter radius.

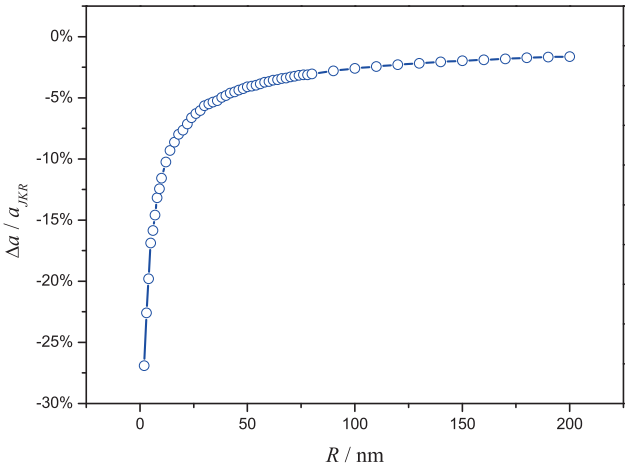

Fig. 8. The variation of the $\Delta a/a_{\mathrm{JKR}}$ with the indenter radius.

$$F_A = f(\sigma_0, \Delta\gamma, E^*, R), \tag{34}$$

$$a_c = g(\sigma_0, \Delta\gamma, E^*, R). \tag{35}$$

Among the four governing parameters, σ_0, $\Delta\gamma$, R and E^*, two of them, namely, R and E^*, have independent dimensions. The dimensions of σ_0, $\Delta\gamma$, F_A and a_c are then given by

$$[\sigma_0] = [R][E^*], \quad [\Delta\gamma] = [R][E^*],$$
$$[F_A] = [R]^2[E^*], \quad [a_c] = [R]. \tag{36}$$

Applying the Π-theorem in dimensional analysis (Barenblatt, 1996), we obtain:

$$\Pi_\alpha = \Pi_\alpha(\Pi_1, \Pi_2), \text{ or equivalently, } F_A = R^2E^*\Pi_\alpha\left(\frac{\Delta\gamma}{RE^*}, \frac{\sigma_0}{RE^*}\right), \tag{37}$$

$$\Pi_\beta = \Pi_\beta(\Pi_1, \Pi_2), \text{ or equivalently, } a_c = R\Pi_\beta\left(\frac{\Delta\gamma}{RE^*}, \frac{\sigma_0}{RE^*}\right), \tag{38}$$

where $\Pi_\alpha = F_A/R^2E^*$, $\Pi_\beta = a_c/R$, $\Pi_1 = \Delta\gamma/RE^*$ and $\Pi_2 = \sigma_0/RE^*$ are all dimensionless.

Based on the above dimensional analysis, we can further draw the scaling laws of the pull-off force and the critical contact radius.

4.2. Linear approximations

A great number of studies have demonstrated that some important properties of nanostructures vary with their geometrical feature size, which is usually called the characteristic size. In this study, the indenter radius (R) can be chosen as the characteristic size. On one hand, when the characteristic size (R) is close to the intrinsic length scale (l_{in}) related to the surface property, the surface effect will become remarkable. On the other hand, when the characteristic size is relatively greater than the intrinsic length scale, the dependence of the corresponding physical properties on the residual surface stress can approximately be linear (Wang et al., 2006).

Therefore, assuming that the pull-off force and the critical contact radius depend linearly on the residual surface stress, i.e., Π_α and Π_β are linear functions of variable Π_2, we have

$$F_A = R^2E^*[\alpha_0(\Pi_1) + \alpha_1(\Pi_1)\Pi_2] = \alpha_0\left(\frac{\Delta\gamma}{RE^*}\right)R^2E^* + \alpha_1\left(\frac{\Delta\gamma}{RE^*}\right)R\sigma_0, \tag{39}$$

where

$$\alpha_0(\Pi_1) = \Pi_\alpha(\Pi_1, 0) \text{ and } \alpha_1(\Pi_1) = \left.\frac{\partial\Pi_\alpha}{\partial\Pi_2}\right|_{\Pi_2=0} \tag{40}$$

are generally functions to be determined by the classical JKR theory and the numerical results. Similarly, the critical contact radius can be written as

$$a_c = R[\beta_0(\Pi_1) + \beta_1(\Pi_1)\Pi_2] = \beta_0\left(\frac{\Delta\gamma}{RE^*}\right)R + \beta_1\left(\frac{\Delta\gamma}{RE^*}\right)\frac{\sigma_0}{E^*}, \tag{41}$$

where

$$\beta_0(\Pi_1) = \Pi_\beta(\Pi_1, 0) \text{ and } \beta_1(\Pi_1) = \left.\frac{\partial\Pi_\beta}{\partial\Pi_2}\right|_{\Pi_2=0}. \tag{42}$$

It should be noted that the intrinsic length scale is $l_{in} = \sigma_0/E^* = 4.59$ nm for polymer EPMD in the present problem; thus, we may conclude that the approximate expressions (39) and (41) are valid when the characteristic size is much greater than the intrinsic length scale ($R \gg l_{in}$).

When the residual surface stresses in Eqs. (39) and (41) are neglected, the pull-off force and the critical contact radius will reduce to the classical results in JKR theory, and we have

$$\alpha_0(\Pi_1)R^2E^* = F_{JKR} = \frac{3}{2}\pi\Delta\gamma R, \tag{43}$$

$$\beta_0(\Pi_1)R = a_{JKR} = \left(\frac{9}{8}\frac{\pi\Delta\gamma R^2}{E^*}\right)^{1/3}. \tag{44}$$

Hence, it can be easily determined that

$$\alpha_0(\Pi_1) = \frac{3}{2}\pi\Pi_1 \text{ and } \beta_0(\Pi_1) = \left(\frac{9\pi}{8}\Pi_1\right)^{1/3}. \tag{45}$$

Next, we are going to determine the explicit forms of the $\alpha_1(\Pi_1)$ and $\beta_1(\Pi_1)$ by numerical analysis. For the pull-off force, the nonlinear relation between the incremental pull-off force ΔF and the indenter radius R are illustrated in Fig. 5. Accordingly, we may assume that $\alpha_1(\Pi_1)$ has the form of the power functions:

$$\alpha_1(\Pi_1) = k_\alpha\Pi_1^n, \tag{46}$$

where k_α and n are real constants. Therefore, Eq. (40) can be rewritten as

$$\Pi_\alpha = \frac{3}{2}\pi\Pi_1 + k_\alpha\Pi_1^n\Pi_2, \tag{47a}$$

or equivalently,

$$F_A = F_{JKR} + k_\alpha\left(\frac{\Delta\gamma}{RE^*}\right)^n R\sigma_0, \tag{47b}$$

where the second term on the right side of Eq. (47b) is the linear correction term due to the surface effect. By taking the common logarithm on both sides of Eq. (47a), we finally obtain

$$\log\Delta\Pi_\alpha = \log(\lambda k_\alpha) + (n+1)\log\Pi_1, \tag{48}$$

where $\Delta\Pi_\alpha = \Pi_\alpha - 3\pi\Pi_1/2$ and $\lambda = \sigma_0/\Delta\gamma$. It is shown obviously in Eq. (48) that $\log\Delta\Pi_\alpha$ depends linearly on $\log\Pi_1$, which denotes a straight line on the two dimensional coordinate plane with the slope of $(n+1)$ and the intercept of $\log(\lambda k_\alpha)$.

The numerical result of the relation between $\log\Delta\Pi_\alpha$ and $\log\Pi_1$ is illustrated in Fig. 9, which does demonstrate that the $\log\Delta\Pi_\alpha - \log\Pi_1$ relation is approximately linear. To ensure the validity of the above the linear approximation, we fit the numerical results in the range of $R > 80$ nm, which are much larger than the intrinsic length scale l_{in}. Therefore, the parameters in Eq. (48) are found to be

$$n + 1 = 1.67 \doteq \frac{5}{3}, \quad \log(\lambda k_\alpha) = -1.027. \tag{49}$$

We can then solve for $n = 2/3$ and $k_\alpha = 1.502 \doteq 3/2$. Hence, the explicit form of the Eq. (47) can be determined as

$$\Pi_\alpha = \frac{3}{2}\pi\Pi_1 + \frac{3}{2}\Pi_1^{2/3}\Pi_2, \tag{50a}$$

or equivalently,

$$F_A = \frac{3}{2}\pi\Delta\gamma R + \frac{3}{2}\left(\frac{\Delta\gamma}{E^*}\right)^{2/3}R^{1/3}\sigma_0, \tag{50b}$$

which indicates that the relation between the pull-off force F_A and the indenter radius R are not linear if the surface effect is considered, and the incremental pull-off force ΔF is proportional to the cube root of the indenter radius. The theoretical curve of this newfound approximation formula is also illustrated in Fig. 5. It is demonstrated that Eq. (50) can give a very accurate estimation of the pull-off force with the surface effect when the indenter radius R is greater than 50 nm.

Notably, as predicted by the conventional theory of adhesive contact (Bradley, 1932; Johnson et al., 1971), the pull-off force is independent on the elastic properties of the bulk materials; however, Eq. (50) reveals that, at the nanoscale, the pull-off force does rely on the equivalent elastic modulus E^*. Therefore, the small-scale adhesive contact is generally more complicated than the macro-adhesive contact, which not only depends on the surface

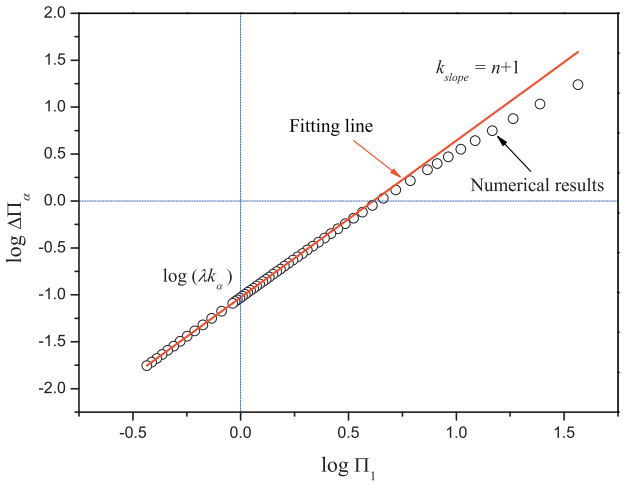

Fig. 9. The fitting line of the Eq. (48).

properties and the geometry of the contacting bodies but also depend on the elastic properties of the bulk materials.

For the critical contact radius a_c under various indenter radii, the relation between the incremental critical radius $\Delta a = a_c - a_{JKR}$ and the indenter radius R is illustrated in Fig. 6. It is shown that the incremental critical radius tends to a constant as the indenter radius R becomes larger. Accordingly, we may conclude that the incremental critical radius is independent on the indenter radius, and hence,

$$\Delta a = \beta_1 \left(\frac{\Delta\gamma}{RE^*}\right)\frac{\sigma_0}{E^*} = const., \tag{51}$$

which implies that β_1 is also a constant function. Thus, Eq. (41) reduces to

$$\Pi_\beta = \left(\frac{9\pi}{8}\Pi_1\right)^{1/3} + k_\beta \Pi_2, \tag{52a}$$

or equivalently,

$$a_c = \left(\frac{9}{8}\frac{\pi\Delta\gamma R^2}{E^*}\right)^{1/3} + k_\beta \frac{\sigma_0}{E^*}, \tag{52b}$$

where k_β is a real constant. Fitting the numerical results in Fig. 6 by employing the least square method, we have $\Delta a = -3.57$ nm and then can determine that $k_\beta = -1.286$. Finally, the explicit form of the Eq. (52) can be determined as

$$\Pi_\beta = \left(\frac{9\pi}{8}\Pi_1\right)^{1/3} - 1.286\Pi_2, \tag{53a}$$

or equivalently,

$$a_c = \left(\frac{9}{8}\frac{\pi\Delta\gamma R^2}{E^*}\right)^{1/3} - 1.286\frac{\sigma_0}{E^*}. \tag{53b}$$

It should be noted that this approximation formula is valid when the indenter radius is greater than 50 nm.

Last but not the least; because the approximation formulas (47) and (52) are constructed using the dimensional analysis and obey the principle of self-similarity, they are universally valid for any material in adhesive contact with a spherical rigid indenter at the nanoscale. In essence, the non-dimensional forms of the formulas (47a) and (52a) are two scaling laws for the adhesive contact with the surface effect, which approximately describes the linear dependence of the pull-off force and the critical contact radius on the residual surface stress.

5. Conclusions

Surface stress and adhesion are two important surface phenomena. In the present paper, both of these effects are considered in the contact problems at the nanoscale, and a generalized JKR adhesive contact model with the surface effect is formulated by employing the non-classical Boussinesq solutions. Some novel points are uncovered. First, the adhesive contact at the nanoscale becomes size dependent; second, the pull-off force is dependent on the elastic constants of the bulk materials. Both of these two interesting phenomena result from the surface stress effect and can be explained by the generalized Young–Laplace equation. The former is due to the curvature-dependence of the surface equilibrium equation and the later is due to the fact that the surface equilibrium is closely related to the elastic properties and stress in the bulk materials. Numerical results show that the effect of surface stress is significant when the indenter radius is less than 20 nm, at which size range the relative errors of the pull-off force and the critical contact radius are approximately 10% and 25%, respectively. Moreover, it is found that the pull-off force depends nonlinearly on the indenter radius, which is different from the classical result, and the variation of the critical contact radius is approximately a constant. Based on the dimensional analysis method, two new scaling laws are proposed to explain these interesting phenomena. These newfound scaling laws are universally valid for any material and characterize the general features of the adhesive contact at the nanoscale.

The contact problems at the nanoscale present many interesting phenomena and fantastic properties. The present work is only a preliminary study and has its limitations, but it lays the foundation for the further study, such as the nano-indentation test for soft materials, the contact between bodies with rough surfaces and the small-scale friction.

Acknowledgements

The authors are grateful for the support from the National Natural Science Foundation of China under Grants #11090330, #11090331 and #11072003. Support from the National Basic Research Program of China (#G2010CB832701) is also acknowledged. The authors also extend their gratitude to the reviewers for their helpful comments.

References

Barenblatt, G.I., 1996. Scaling, Self-similarity, and Intermediate Asymptotics. Cambridge University Press, Cambridge.
Barthel, E., 2008. Adhesive elastic contacts: JKR and more. J. Phys. D: Appl. Phys. 41, 163001.
Bradley, R.S., 1932. The cohesive force between solid surfaces and the surface energy of solids. Philos. Mag. 13, 853–862.
Cammarata, R.C., 1994. Surface and interface stress effects in thin films. Prog. Surf. Sci. 46, 1–38.
Chen, C.Q., Shi, Y., Zhang, Y.S., Zhu, J., Yan, Y.J., 2006. Size dependence of Young's modulus of ZnO nanowires. Phys. Rev. Lett. 96, 075505.
Chen, S.H., Gao, H., 2007. Bio-inspired mechanics of reversible adhesion: orientation-dependent adhesion strength for non-slipping adhesive contact with transversely isotropic elastic materials. J. Mech. Phys. Solids 55, 1001–1015.
Chen, S.H., Yan, C., Soh, A.K., 2009a. Adhesive behavior of two-dimensional power-law graded materials. Int. J. Solids Struct. 46, 3398–3404.
Chen, S.H., Yan, C., Zhang, P., Gao, H., 2009b. Mechanics of adhesive contact on a power-law graded elastic half-space. J. Mech. Phys. Solids 57, 1437–1448.
Chhapadia, P., Mohammadi, P., Sharma, P., 2011. Curvature-dependent surface energy and implications for nanostructures. J. Mech. Phys. Solids 59, 2103–2115.

Dai, S.X., Gharbi, M., Sharma, P., Park, H.S., 2011. Surface piezoelectricity: size effects in nanostructures and the emergence of piezoelectricity in non-piezoelectric materials. J. Appl. Phys. 110, 104305.
Dai, S.X., Park, H.S., 2013. Surface effects on the piezoelectricity of ZnO nanowires. J. Mech. Phys. Solids 61, 385–397.
Derjaguin, B.V., Muller, V.M., Toporov, Y.P., 1975. Effect of contact deformations on the adhesion of particles. J. Colloid Interface Sci. 53, 314–326.
Dingreville, R., Qu, J., Cherkaoui, M., 2005. Surface free energy and its effect on the elastic behavior of nano-sized particles, wires and films. J. Mech. Phys. Solids 53, 1827–1854.
Dingreville, R., Qu, J., 2008. Interfacial excess energy, excess stress and excess strain in elastic solids: planar interfaces. J. Mech. Phys. Solids 56, 1944–1954.
Duan, H.L., Wang, J., Huang, Z.P., Karihaloo, B.L., 2005a. Eshelby formalism for nano-inhomogeneities. Proc. R. Soc. A 461, 3335–3353.
Duan, H.L., Wang, J., Huang, Z.P., Karihaloo, B.L., 2005b. Size-dependent effective elastic constants of solids containing nano-inhomogeneities with interface stress. J. Mech. Phys. Solids 53, 1574–1596.
Feng, G., Nix, W.D., 2004. Indentation size effect in MgO. Scr. Mater. 51, 599–603.
Gao, X., Hao, F., Fang, D.N., Huang, Z.P., 2013. Boussinesq problem with the surface effect and its application to contact mechanics at the nanoscale. Int. J. Solids Struct. 50, 2630–2630.
Grierson, D.S., Liu, J.J., Carpick, R.W., Turner, K.T., 2013. Adhesion of nanoscale asperities with power-law profiles. J. Mech. Phys. Solids 61, 597–610.
Gurtin, M.E., Murdoch, A.I., 1975. A continuum theory of elastic material surfaces. Arch. Ration. Mech. Anal. 57, 291–323.
Gurtin, M.E., Murdoch, A.I., 1978. Surface stress in solids. Int. J. Solids Struct. 14, 431–440.
Huang, Z.P., Wang, J., 2006. A theory of hyperelasticity of multi-phase media with surface/interface energy effect. Acta Mech. 182, 195–210 (Erratum: Acta Mech. 215, 365–366.).
Huang, Z.P., Sun, L., 2007. Size-dependent effective properties of a heterogeneous material with interface energy effect: from finite deformation theory to infinitesimal strain analysis. Acta Mech. 190, 151–163 (Erratum: Acta Mech. 215, 363–364.).
Huang, Z.P., Wang, J., 2013. Micromechanics of nanocomposites with interface energy effect. In: Li, S.F., Gao, X.L. (Eds.), Handbook of Micromechanics and Nanomechanics. Pan Stanford Publishing Pte Ltd., Singapore, pp. 303–348.
Jing, G.Y., Duan, H.L., Sun, X.M., Zhang, Z.S., Xu, J., Li, Y.D., Wang, J.X., Yu, D.P., 2006. Surface effects on elastic properties of silver nanowires: contact atomic-force microscopy. Phys. Rev. B 73, 235409.
Johnson, K.L., Kendall, K., Roberts, A.D., 1971. Surface energy and the contact of elastic solids. Proc. R. Soc. Lond. A 324, 301–313.
Johnson, K.L., 1985. Contact Mechanics. Cambridge University Press, London.
Long, J.M., Wang, G.F., Feng, X.Q., Yu, S.W., 2012. Two-dimensional Hertzian contact problem with surface tension. Int. J. Solids Struct. 49, 1588–1594.
Long, J.M., Wang, G.F., 2013. Effects of surface tension on axisymmetric Hertzian contact problem. Mech. Mater. 56, 65–70.
Maugis, D., 1992. Adhesion of spheres — the JKR–DMT transition using a Dugdale model. J. Colloid Interface Sci. 150, 243–269.
Ma, Q., Clarke, D.R., 1995. Size dependent hardness of silver single-crystals. J. Mater. Res. 10, 853–863.
Mark, J.E., 2009. Polymer Data Handbook, second ed. Oxford University Press, New York.
Medasani, B., Vasiliev, I., 2009. Computational study of the surface properties of aluminum nanoparticles. Surf. Sci. 603, 2042–2046.
Miller, R.E., Shenoy, V.B., 2000. Size-dependent elastic properties of nanosized structural elements. Nanotechnology 11, 139–147.
Mohammadi, P., Sharma, P., 2012. Atomistic elucidation of the effect of surface roughness on curvature-dependent surface energy, surface stress and elasticity. Appl. Phys. Lett. 100, 133110.
Mohammadi, P., Liu, L.P., Sharma, P., Kukta, R.V., 2013. Surface energy, elasticity and the homogenization of rough surfaces. J. Mech. Phys. Solids 61, 325–340.
Park, H.S., Klein, P.A., 2008. Surface stress effects on the resonant properties of metal nanowires: the importance of finite deformation kinematics and the impact of the residual surface stress. J. Mech. Phys. Solids 56, 3144–3166.
Popov, V.L., 2010. Contact Mechanics and Friction: Physical Principles and Applications. Springer-Verlag, Berlin.
Povstenko, Y.Z., 1993. Theoretical investigation of phenomena caused by heterogeneous surface-tension in solids. J. Mech. Phys. Solids 41, 1499–1514.
Schwarz, U.D., 2003. A generalized analytical model for the elastic deformation of an adhesive contact between a sphere and a flat surface. J. Colloid Interface Sci. 261, 99–106.
Sharma, P., Ganti, S., 2004. Size-dependent Eshelby's tensor for embedded nano-inclusions incorporating surface/interface energies. J. Appl. Mech. 71, 663–671.
Sun, C.T., Wang, Y., Tay, B.K., Li, S., Huang, H., Zhang, Y.B., 2002. Correlation between the melting point of a nanosolid and the cohesive energy of a atom. J. Phys. Chem. B 106, 10701–10705.
Tabor, D., 1977. Surface forces and surface interactions. J. Colloid Interface Sci. 53, 2–13.
Wang, J., Duan, H.L., Huang, Z.P., Karihaloo, B.L., 2006. A scaling law for properties of nano-structured materials. Proc. R. Soc. A 462, 1355–1363.
Wang, G.F., Feng, X.Q., 2007. Effects of surface stresses on contact problems at nanoscale. J. Appl. Phys. 101, 013510.
Weissmuller, J., Duan, H.L., 2008. Cantilever bending with rough surfaces. Phys. Rev. Lett. 101, 146102.
Zhao, Y.P., Wang, L.S., Yu, T.X., 2003. Mechanics of adhesion in MEMS — a review. J. Adhes. Sci. Technol. 17, 519–546.
Zhao, X.J., Rajapakse, R.K.N.D., 2009. Analytical solutions for a surface-loaded isotropic elastic layer with surface energy effects. Int. J. Eng. Sci. 47, 1433–1444.
Zhang, W.X., Wang, T.J., Chen, X., 2010. Effect of surface/interface stress on the plastic deformation of nanoporous materials and nanocomposites. Int. J. Plast. 26, 957–975.
Zheng, Z.J., Yu, J.L., 2007. Using the Dugdale approximation to match a specific interaction in the adhesive contact of elastic objects. J. Colloid Interface Sci. 310, 27–34.